Journal of Superconductivity and Novel Magnetism (2018) 31:3889–3898
https://doi.org/10.1007/s10948-018-4692-x

ORIGINAL PAPER

Comparing the Effects of Nb, Pb, Y, and La Replacement on the Structural, Electrical, and Magnetic Characteristics of Bi-Based Superconductors

Reza Asghari[1,2] · Hamid Naghshara[1] · Leyla Çolakerol Arsalan[3] · Hasan Sedghi[2]

Received: 23 March 2018 / Accepted: 6 April 2018 / Published online: 28 April 2018

Abstract

In this study, the effects of Pb, Nb, La, and Y replacements were investigated on Bi-based superconducting materials. In preparing the samples, we used a method called solid-state reaction method. The patterns of the X-ray diffraction of all samples indicated presence of Bi-2212 and Bi-2223 phases. The results obtained from XRD revealed that with increase of the melting point of substation elements, the Bi-2223 phase decreased while the Bi-2212 phase and impurity phases of samples grew. From the electrical resistivity measurements using the four-probe method, it was found that sample A with Pb and sample B with La replacements had the maximum and minimum critical temperatures of 111.4 and 81.6 K, respectively. Based on hysteresis loop (M–H) measurement using Bean's model, estimation of critical current density (J_c) showed that sample A with Pb and sample B with La substitution had the maximum and minimum values respectively. These results may be due to the melting point of these elements with values of 888, 1512, 2315, and 2425 °C for PbO, Nb_2O_5, La_2O_3, and Y_2O_3, respectively. These elements were replaced by Bi_2O_3 with a melting point of 817 °C. Further, the samples were prepared at the temperature of 845 °C. It seems at this temperature, these elements not only dissolve within the main matrix and participate in the formation of the Bi-2212 phase during the sintering process but they also participate in the development of the variety of the impurity phases as confirmed by XRD results.

Keywords Bi-based superconductors · Volume fraction · Critical temperature · Four-point probe method · Lattice parameters · p parameter

1 Introduction

Addition or substitution in Bismuth-based superconductors as a probe is used for determining whether they exhibit better superconductivity properties or not. Since the time Bi-based superconductors have been discovered [1], a great deal of research has been done by researchersfrom all over the world [2–10]. The researchers have been trying to improve the superconductive properties and better understand the structural characteristics of the superconductors. Activities such as substitution and addition of a variety of elements have done by researchers, to determine whether the superconductivity properties of this type of HTSC improve or worsen. BSSCO is the abbreviations of the Bi-based superconductors defined by the $Bi_2Sr_2Ca_{n-1}Cu_nO_{2n+4+y}$ general composition where n is the number of CuO_2 layers in the crystal structure. In this composition, the values of n are 1, 2 and 3. Regarding the values of n, Bi-based superconductors are characterized by three phases, called Bi-2201 phase, Bi-2212 phase and Bi-2223 phase with the critical temperature of 20, 85, and 110 K, respectively [11–13]. Smrckova et al. indicated that the Bi-2223 phase with the chemical formula

✉ Reza Asghari
rasghari1356@gmail.com

1 Department of Condensed Matter, Faculty of Physics, University of Tabriz, Tabriz, Iran

2 Department of Physics, Superconductivity Research Center, University of Urmia, Urmia, Iran

3 Department of Physics, Gebze Technical University, Cayirova, Kocaeli 41400, Turkey

of $Bi_2Sr_2Ca_2Cu_3O_{10+y}$ is suitable to be used practically in superconducting devices with liquid nitrogen temperature ($T > 77$ K) [14]. In spite of many attempts and works to reach the Bi-2223 single phase, preparing Bi-based superconducting system leads to the coexistence of Bi-2223 and Bi-2212 along with some impurity phases. In a BSCCO system, the superconductive characteristics depend on the characteristics of the elements in the structure of the crystal. Researchers have found that lead (Pb) replacement improves the superconductive characteristics of the BSCCO system. It means that lead is the most significant replacement element among other elements. The presence of Pb in the BSCCO system, helps the reaction kinetics of the Bi-2223 phase. The results of substituting Pb with Bi in preparing the BSCCO system with the formula of $Bi_{2-x}Pb_xSr_2Ca_2Cu_3O_\delta$ by the minimum amount of Pb (x) have indicated that $x = 0.3$ to 0.4. For this reason, many researchers have selected Pb content (x) with an amount of 0.4 for preparing the samples [15–17]. Li et al. investigated the effect of the cations with high valency such as Ta^{+5}, V^{+5}, and Nb^{+5} on the formation of the Bi-2223 phase. They found that the formation of Bi-2223 phase can significantly improve with doping any one of these elements [18]. Ghazanfari et al. found that partial addition of niobium (Nb) does not enhance the formation of Bi-2223 phase but improves the connectivity between grains and the critical current density (J_c) in the BSCCO system [19]. Ekicibil et al. examined the role of Pb replacement with Gd in the BSCCO system with the composition of $Bi_{1.7}Pb_{0.35-x}Gd_xSr_2Ca_3Cu_4O_{12+y}$. Their results revealed that formation of the Bi-2223 phase decreases with increasing the Gd substitution. Also, the insulating phases grow

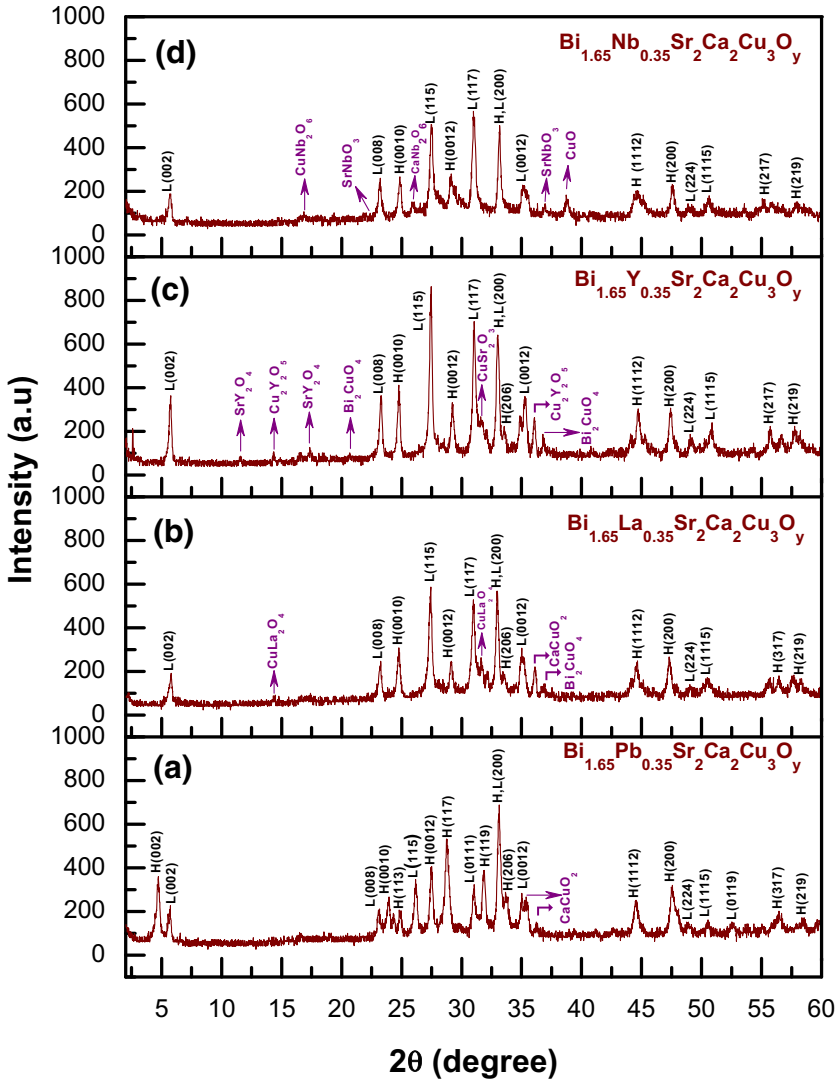

Fig. 1 Patterns of the XRD (Samples A to D)

as well. In other words, superconducting characteristics elevating Pb^{+2} replacement with Gd^{+3} [20].

In previous studies, we investigated the Pb replacement with Nb in the BSCCO system with a nominal composition of $Bi_{1.65}Pb_{0.35-x}Nb_xSr_2Ca_2Cu_3O_{10+\delta}$ ($x = 0.0, 0.05, 0.1,$ 015, 0.2, 0.25, 0.3, and 0.35). The results revealed that with enhancing Pb substitution by Nb content the volume fraction of the low-T_c (Bi-2212) phase and impurity phases increased. Moreover, with elevation of the Nb content, the critical temperature $\left(T_c^{\text{offset}}\right)$ and the density of critical current (J_c) of the samples declined. In other words, the superconducting properties of the samples degrades by replacing niobium [21, 22].

As noted above, in Bismuth-based superconductors, Pb replacement improves the superconducting characteristics. In this study, the aim is to compare the effects of Pb, Nb, La, and Y replacements on the structural and physical properties of the BSSCO system with the general formula of $Bi_{1.65}X_{0.35}Sr_2Ca_2Cu_3O_{10+\delta}$ (X = Pb, Nb, La, and Y).

2 Experimental

BSCCO samples with the chemical composition of $Bi_{1.65}X_{0.35}Sr_2Ca_2Cu_3O_{10+\delta}$ (X = Pb, Nb, La, and Y) were prepared from high-purity degree powders of $SrCO_3$ (99.99%), Bi_2O_3 (99.99%), $CaCO_3$ (99.99%), Nb_2O_5 (99.99%) PbO (99.99%), Y_2O_3, La_2O_3, and CuO (99.99%) by through solid-state reaction method [23]. The required quantities of the materials in stoichiometric proportions were weighted and mixed (the powders were mixed nearly for 1 h) after the precursors came in pill form and calcined in air at 810 °C for 48 h at an optimized heating rate of 5 °C. Similar to the first step, for the second time, the samples were sintered at 825 °C in the air for 48 h. For preparing of the pellets from powders, we pressed the pellets at 250 MPa in calcination processes and further pressed at 450 MPa in the final process to a circular shape with 2 mm thickness and 13 mm diameter. Finally, the samples (pellets) were sintered at 845 °C at an optimized heating rate of 5 °C for 100 h. In this research, we labeled our samples as A, B, C, and D.

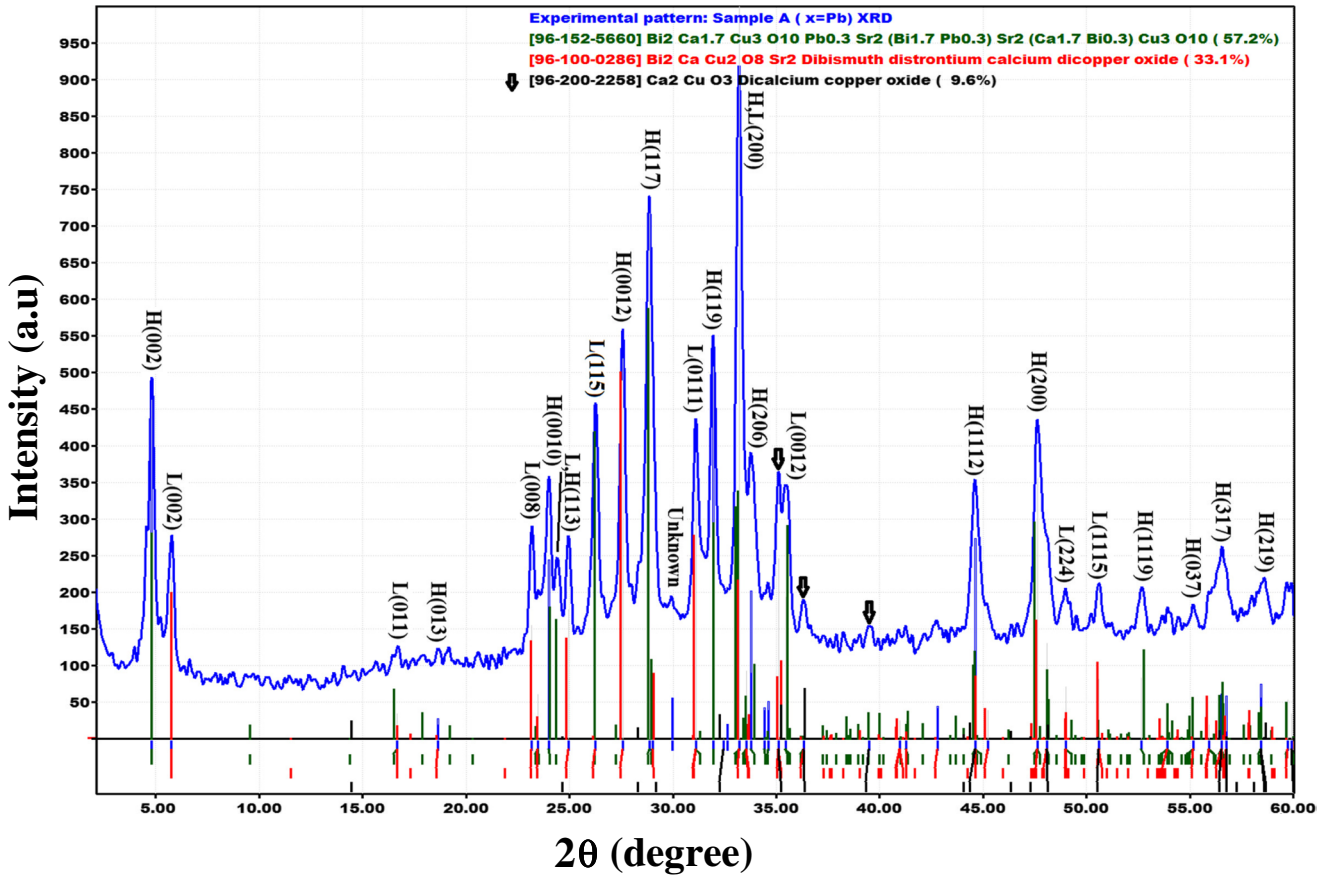

Fig. 2 Detected phases of sample A

In order to identify the phases present in the materials and determine the lattice parameters, X-ray diffraction of the sample was checked by SIMENS X-ray diffractometer with CuK_{α} radiation (1.5406 Å) within the range of $2\theta = 2$–60°. Calculation of unit cell parameters was done using Match 3.3 software. Measurements of the DC resistivity of the samples (R–T) were done by the standard 4point probe method. Also, we measured the magnetic properties of the samples by a VSM. The SEM images for analyzing of the microstructure of the samples were prepared by MIRA3 TESCAN.

3 Results and Discussion

Figure 1 demonstrates the XRD patterns of $Bi_{1.65}X_{0.35}Sr_2Ca_2Cu_3O_{10+\delta}$ (X = Pb, Nb, La, and Y) samples. The peaks of samples are indexed with Bi-2223(H) and Bi-2212 (L) as well as their Miller indices. Our results indicated that all samples had two phases of Bi-2212, Bi-2223, and various non-superconducting impurity phases. Non-superconducting impurity phases such as $CaCuO_2$, CuO, $CuLa_2O_4$, Ca_2CuO_3, $BiCuO_4$, SrY_2O_4, $Cu_2Y_2O_5$, $CuSr_2O_3$, $Ca_2Y_2O_5$, $CuNb_2O_6$, $CaNb_2O_6$, and $SrNbO_3$ were detected at the diffraction angle of 2θ = 2–60°. The present phases of the samples were detected using the Match 3.3 software, as indicated in Figs. 2, 3, 4, and 5. In sample A with Pb (melting point = 888 °C) replacement, only the impurity phase of $CaCuO_2$ was observed. In addition, for samples D, C, and B with elevation of the melting point of substitution elements, various non-superconducting impurity phases were observed. At $2\theta = 4.7°$, the intensity of $H(002)$ peak, at $2\theta = 24.7°$, the intensity of $H(113)$ and $H(0012)$ peaks at $2\theta = 28.7°$, and the intensity of $H(119)$ peak at $2\theta = 31.8°$, which belong to the Bi-2223 phase, and with increasing of the melting point of substitution elements in samples B, C, and D, these peaks disappear. Moreover, at $2\theta = 5.7°$the intensity of $L(002)$ peak which belongs to the Bi-2212 phase grows, with raising the melting point of the substitution elements. The highest value for the intensity of $L(002)$ peak is seen in sample C with yttrium (melting point = 2425 °C) substitution. From the XRD peaks and using the d-values along with (hkl) reflections of the X-ray diffraction pattern, the lattice parameters of samples,

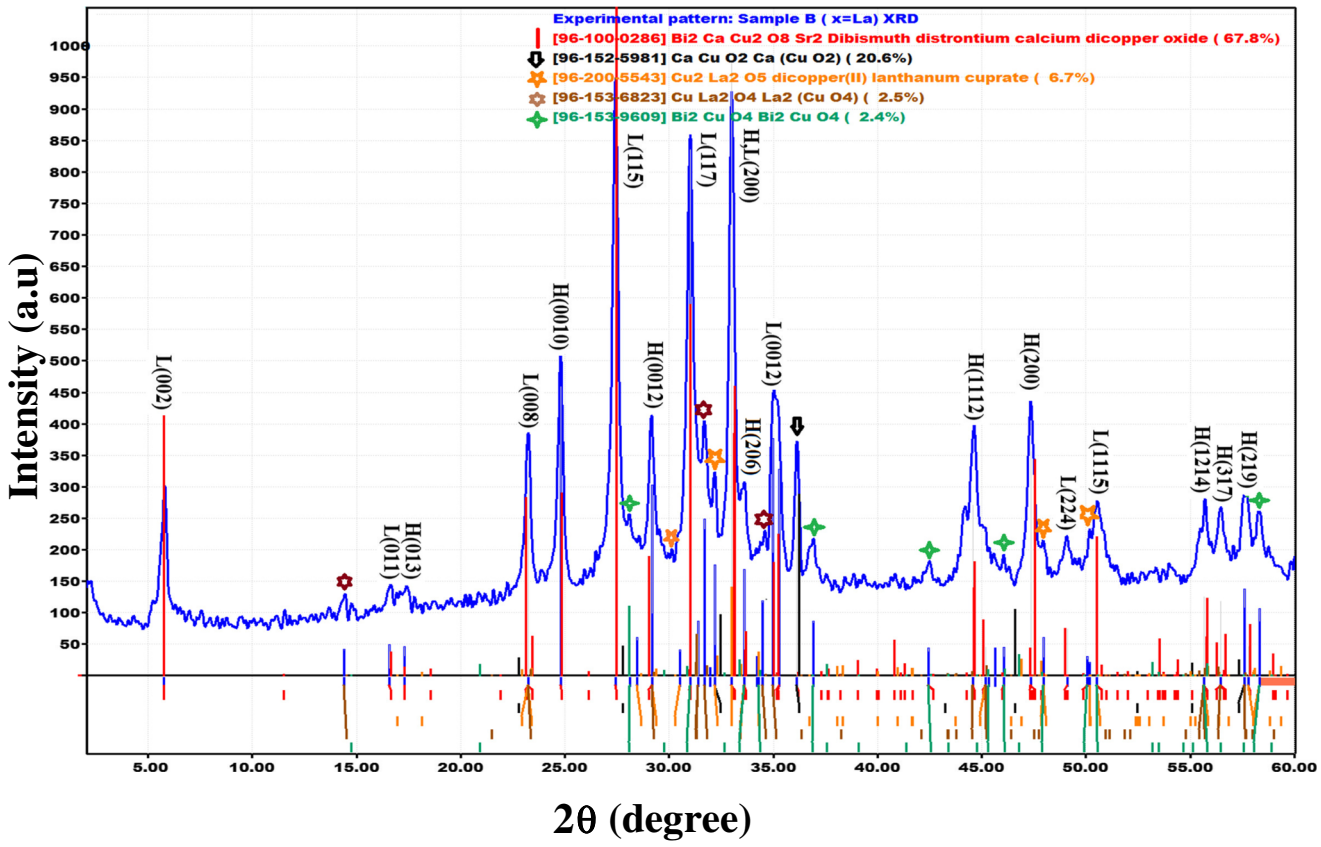

Fig. 3 Detected phases of sample B

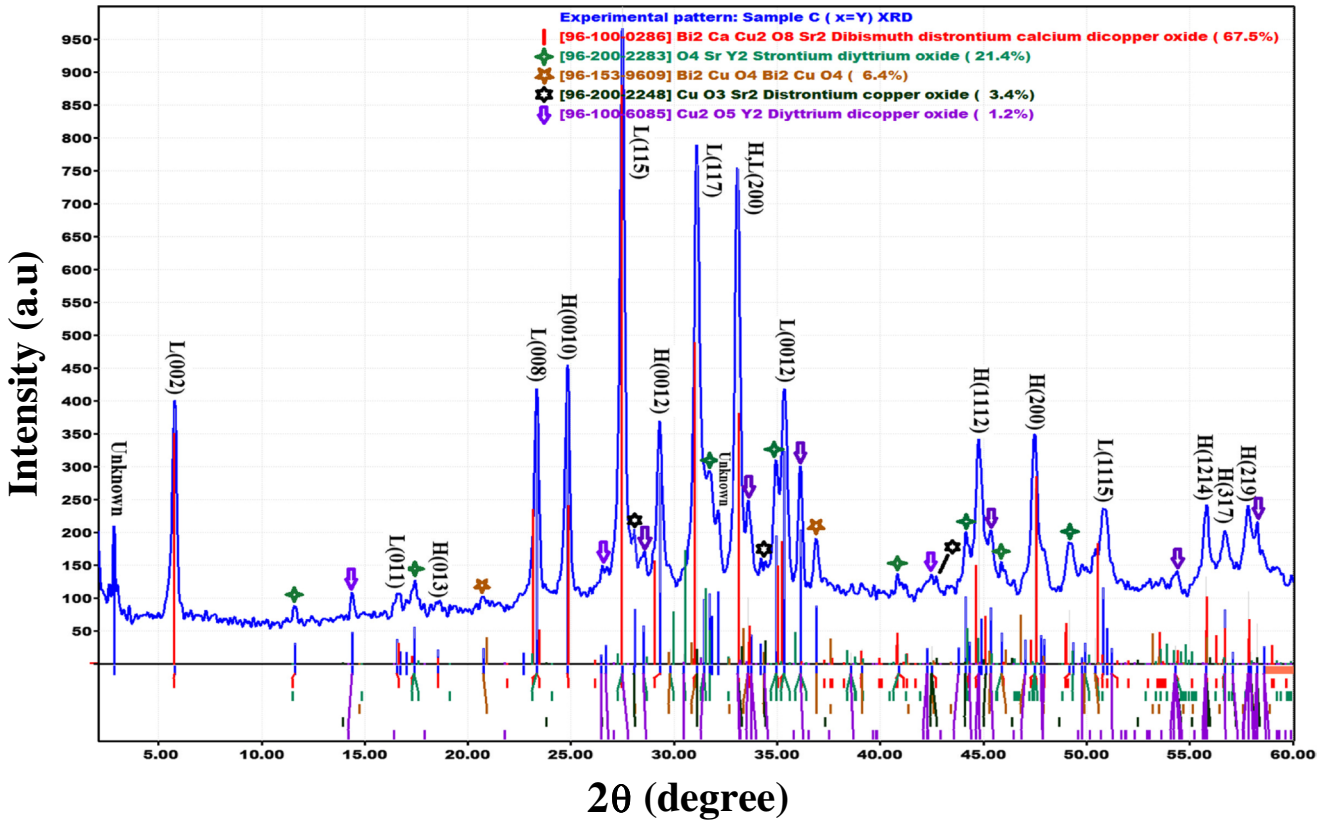

Fig. 4 Detected phases of sample C

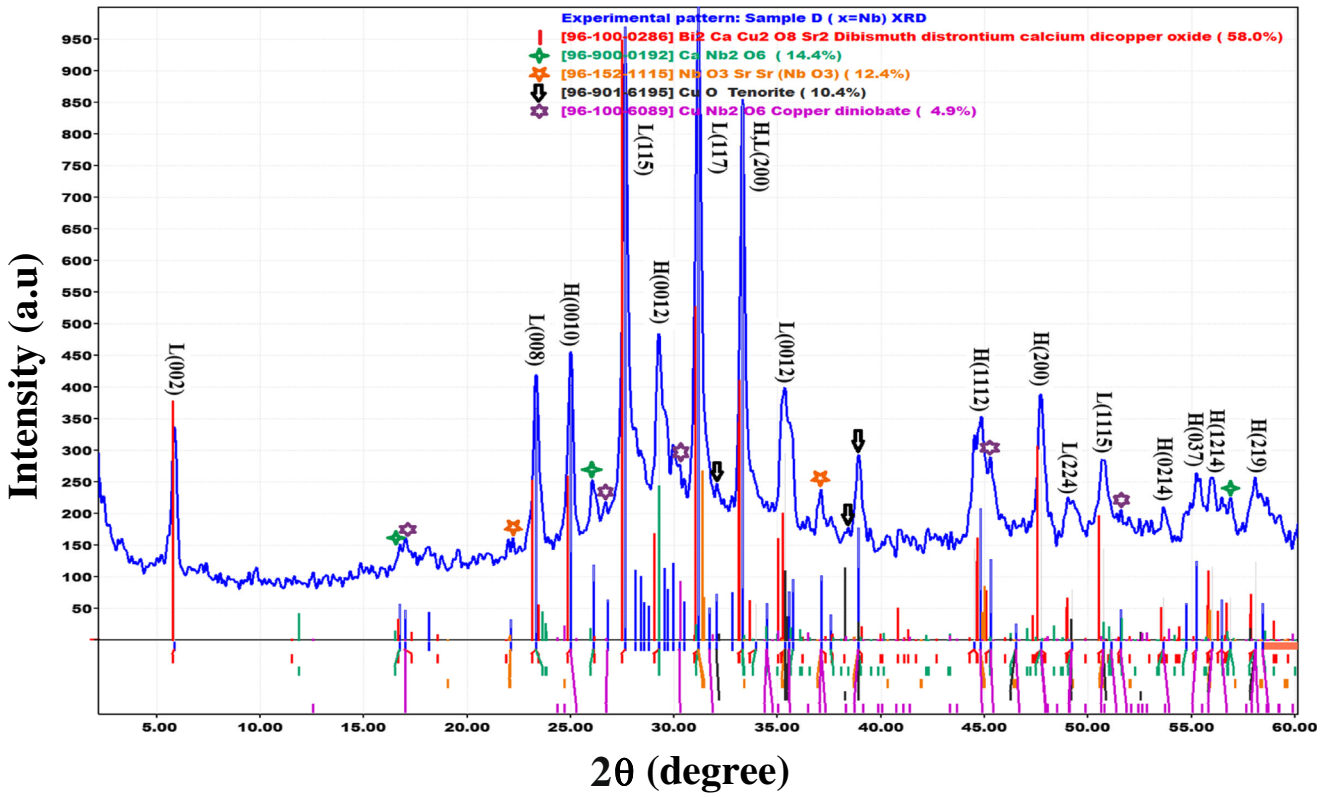

Fig. 5 Detected phases of sample D

were calculated by Match 3.3 software as indicated in Table 1. The results obtained for lattice parameters, revealed orthorhombic structure for crystalline symmetry of the samples. This crystalline symmetry of BPSCCO system has a good agreement with the findings in previous studies [24, 25]. However, in the calculated lattice parameters according to the different replacement of the elements, no significant order was observed.

The volume fraction of the phases was calculated using the corresponding XRD peaks and the following equations [26, 27]:

$$\mathrm{Bi2223}(\%) \approx \frac{\Sigma \mathrm{I}\,(\mathrm{Bi}-2223)}{\Sigma \mathrm{I}\,(\mathrm{Bi}-2223)+\Sigma \mathrm{I}\,(\mathrm{Bi}-2212)+\Sigma \mathrm{I}\,(\mathrm{impurity})} \times 100 \quad (1)$$

$$\mathrm{Bi2212}(\%) \approx \frac{\Sigma \mathrm{I}\,(\mathrm{Bi}-2212)}{\Sigma \mathrm{I}\,(\mathrm{Bi}-2223)+\Sigma \mathrm{I}\,(\mathrm{Bi}-2212)+\Sigma \mathrm{I}(\mathrm{impurity})} \times 100 \quad (2)$$

$$\mathrm{Impurity}(\%) \approx \frac{\Sigma \mathrm{I}\,(\mathrm{impurity})}{\Sigma \mathrm{I}\,(\mathrm{Bi}-2223)+\Sigma \mathrm{I}\,(\mathrm{Bi}-2212)+\Sigma \mathrm{I}\,(\mathrm{impurity})} \times 100 \quad (3)$$

where, I (Bi-2223), I (Bi-2212), and I (impurity) represent the intensity of the phases (Fig. 1). The volume fraction of the phases of the different samples is provided in Table 1. From this table, it can be observed that the samples D, C, B, and A contained 36.73, 33.69, 37.86, and 54.05% of the Bi-2223 phase and 12.54, 15.56, 13.86, and 6.48% of the impurity phases, respectively. Also, the results demonstrated that with elevation of the melting point of the substitution elements in the system, the percentage volume fraction of the impurity phases increased. It can be concluded that substitution of the high melting point elements in the BSCCO system is the main reason for increased impurity phases in the samples. These elements not only dissolve completely within the main matrix during the sintering process, they also cause the development of the various non-superconducting phases.

Table 1 The volume fraction of the samples phases

Sample	Bi-2223 (%)	Bi-2212 (%)	Impurity (%)
A (Pb substitution)	54.05	39.47	6.48
B (La substitution)	37.86	48.28	13.86
C (Y substitution)	33.69	50.75	15.56
D (Nb substitution)	36.73	50.73	12.54

Figure 6 illustrates R–T curves of the samples from the temperatures of 110 down to 10 K. In this figure, the resistivity decreases with temperature reduction. This characteristic exhibited metallic behavior for all samples. The resistivities corresponding to the onset critical temperatures of samples D, C, B, and A were 0.0027, 0.0112, 0.0083, and 0.0029 ohm cm, respectively. Sample D with Nb substitution had the lowest resistivity. The values of the T_c^{offset}, T_c^{onset}, and transition temperature width $\Delta T_c = T_c^{\mathrm{offset}} - T_c^{\mathrm{onset}}$ for all samples are presented in Table 2. Transition temperature width (ΔT_c) is another physical property, which should be narrowed in a good superconductor. The maximal narrow transition width was observed in sample A with Pb substitution. Further, among the samples, Sample B with La substitution had the lowest T_c^{offset} ($R = 0$) with the value of 20.7 K. The most dramatic reduction of the onset critical temperature $\left(T_c^{\mathrm{onset}}\right)$ was seen in samples B and C. The reason for this could be attributed to the melting point of these elements (2315 and 2425 °C for La_2O_3 and Y_2O_3), respectively. These elements were substituted by Bi_2O_3 with a melting point of 817 °C. In this research, the samples were prepared at 845 °C. It seems that at this temperature, these elements were not well melted and did not replaced bismuth.

M–T curves of the samples were obtained at the external magnetic field of 50 Oe as displayed in Fig. 7. Diamagnetic behavior was observed across all samples below T_c^{onset}. The maximum and minimum diamagnetic properties were observed in the samples with Pb and Y substitutions, respectively. Furthermore, it can be noticed that the samples

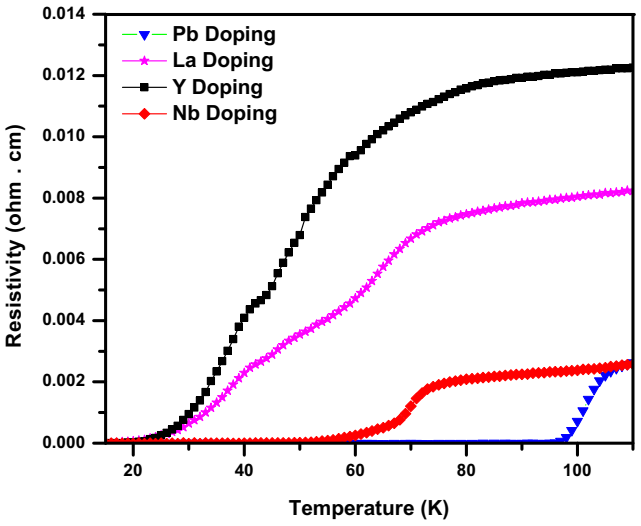

Fig. 6 R–T curves of the samples

Table 2 Summary of the resistivity, critical temperature (T_c^{offset}, T_c^{onset}), transition width (ΔT_c), and cell parameters of samples

Sample	ρ_{R-T}(ohmcm)	T_c^{offset} (K)	T_c^{onset} (K)	a (Å)	b (Å)	c (Å)
A (Pb substitution)	0.0029	95.1	111.4	5.3881	5.3273	30.7238
B (La substitution)	0.0083	20.7	81.6	5.4216	5.4179	30.6326
C (Y substitution)	0.0112	22.3	89.9	5.4106	5.4057	30.4406
D (Nb substitution)	0.0027	50.3	107.9	5.4054	5.4021	30.6965

with Pb and Nb substitutions having a lower melting point showed narrower a superconducting phase transition width.

Another important factor in characterizing superconductors is the DC hysteresis cycles. Using this factor, we can determine the critical current density (J_c). Therefore, we measured this factor at the temperature of 10 K under magnetic field ranging from − 9000 to + 9000 Oe. The obtained results are demonstrated in Fig. 8. The diamagnetic behavior of our samples is in good agreement with the conventional type-II superconductivity. Further, J_c of the samples was obtained by the Bean's critical state model [28] and using the hysteresis loops. According to this model, J_c is proportional to the hysteresis loop width($\Delta M = |M_+ - M_-|$) and is described by the following relation:

$$J_c = 20\frac{|\Delta M|}{a\left(1-\frac{b}{3a}\right)} \quad (4)$$

where J_c is in amperes per square centimeter, and M_+ and M_- are the maximum magnetizations of the M–H loops for negative and positive applied magnetic fields, respectively. ΔM (regarding electromagnetic units per cubic centimeter) is the absolute difference among magnetization values, which are recorded at the same increasing and decreasing field branches. Also, b and a ($b<a$) represent the sample dimensions. Figure 9 illustrates the J_c–H curves of the samples. As can be seen from this figure and Table 3, sample A with Pb substitution and sample C with Y substitution have larger $\left(=4.60\times10^3\,\frac{A}{cm}^2\right)$ and smaller $\left(=1.92\times10^2\,\frac{A}{cm^2}\right)$ values compared with the other samples, respectively. This result is due to the formation of fewer and more non-superconducting impurity phases in samples A and C, respectively.

The grain structure is also one of the most significant factors in high-temperature superconductors which can be determined by SEM images. Figure 10 displays the SEM images for all samples. Large randomly distributed plate-like crystal structures are evident in this figure. This is the total characteristics of the glass-ceramic materials as reported by other researchers [29, 30]. In spite of some pores among the grains, the compact ratio of the samples will result in a favorable critical current density which is of great importance in high-temperature ceramic superconductors. Furthermore, the images indicate that the size and distribution of the plate-like grains on the surface of the samples are different. According to a research done by Tampieri et al., the Bi-2212 phase has higher crystallographic density and more pores than the Bi-2223

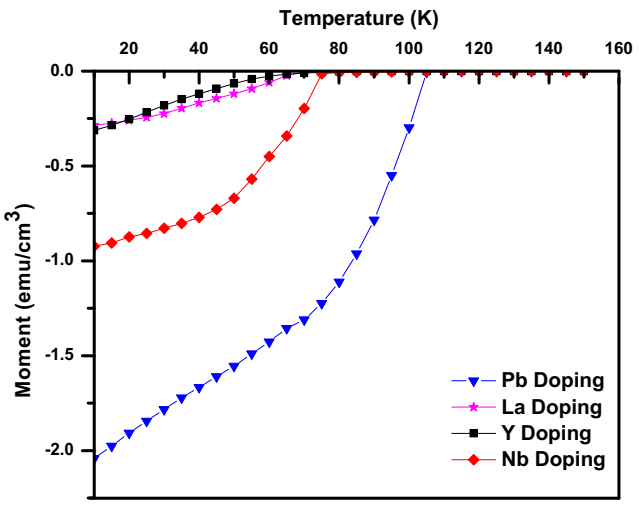

Fig. 7 M–T curves at an applied magnetic field of 50 Oe

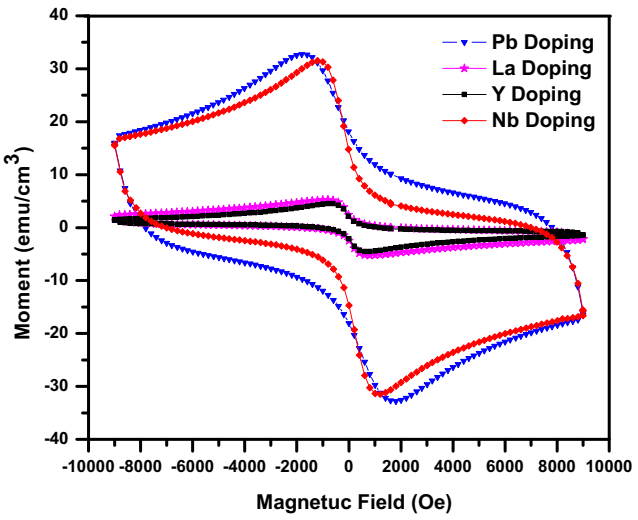

Fig. 8 M–H curves at the temperature of 10 K

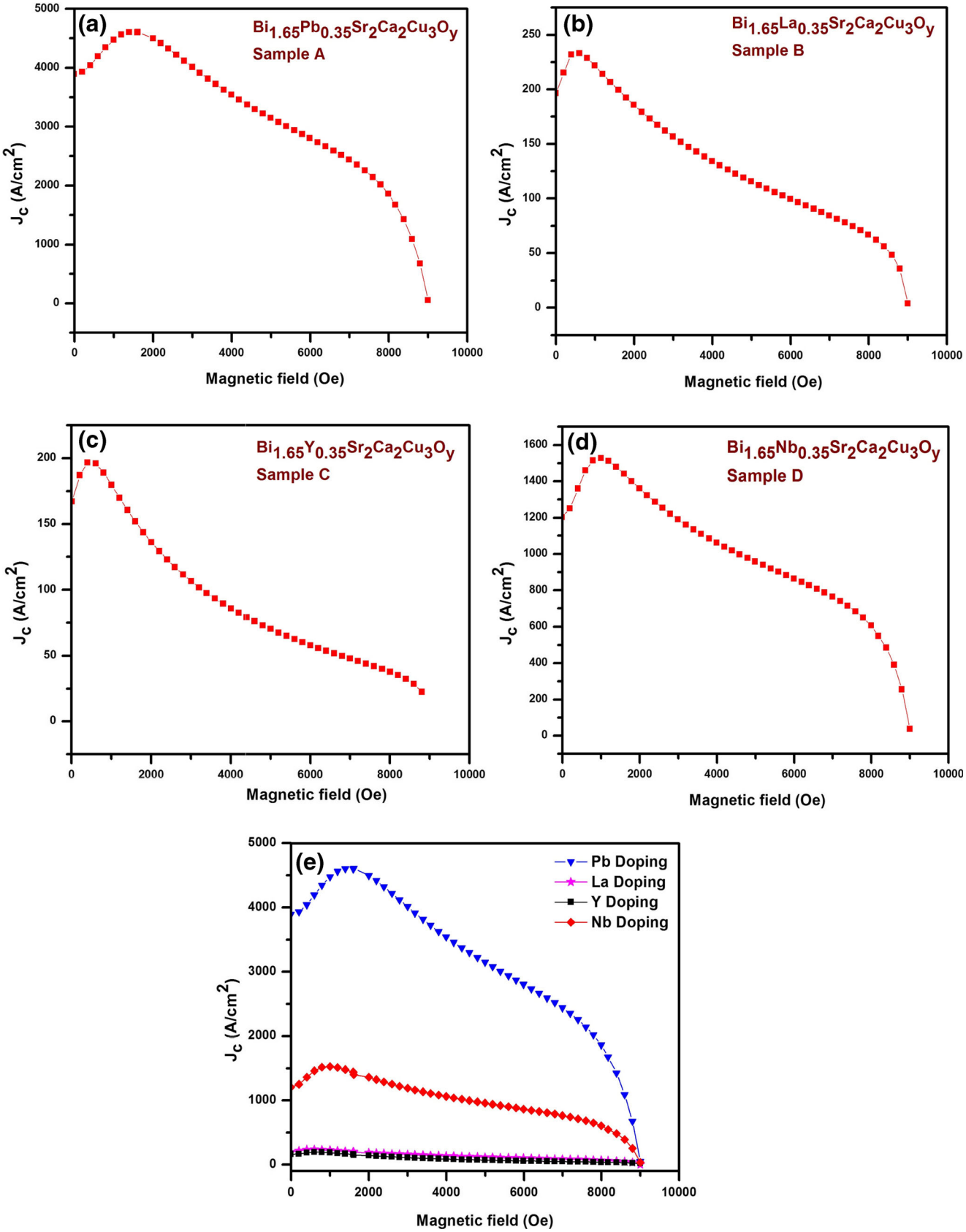

Fig. 9 J_c–H curves of the samples

Table 3 Summary of the critical current density

Sample	ΔM	$J_c\left(\frac{A}{cm^2}\right)$	p values
A (Pb substitution)	42.89	4.60×10^3	0.119
B (La substitution)	2.18	2.33×10^2	0.061
C (Y substitution)	1.86	1.96×10^2	0.062
D (Nb substitution)	14.04	1.53×10^3	0.076

[31]. Based on the above-mentioned reference, sample B with La and sample C with Y replacements have higher crystallographic density and more pores. In other words, in these samples, the values of Bi-2212 phase are higher than those of others, as confirmed by the XRD results. Moreover, from Fig. 10b, c, it can be observed that the surface structure of the samples contains partially molten regions. Also, with elevation of the melting point of the substitution elements, the microstructure of the sample deteriorates and the number of molten regions increases.

Superconducting transition temperature has a parabolic relationship with the hole concentration p (the number of holes per copper atom). p parameter is calculated by the following equation [32]:

$$p = \left(\frac{1}{82.6}\left(1 - \frac{T_c}{T_c^{max}}\right)\right)^{\frac{1}{2}} + 0.16 \quad (5)$$

where T_c^{max} is 110 K for the Bi-2223 system. Many researchers used this equation for the BSCCO system. According to previous works [33–35], the p parameter for the unsubstituted Bi-2223 ranges between 0.115 and 0.161. In this research, p values of the samples D, C, B, and A were calculated as 0.079, 0.062, 0.061, and, 0.119 respectively. All samples except the sample with Pb replacement had lower values compared with previous calculations. The obtained results indicated that replacement of Bi^{+3} by Y^{+3}, La^{+3}, and Nb^{+5} causes reduced Bi-2223 phase and the emergence of other phases. The results of the p values confirm the XRD and SEM results.

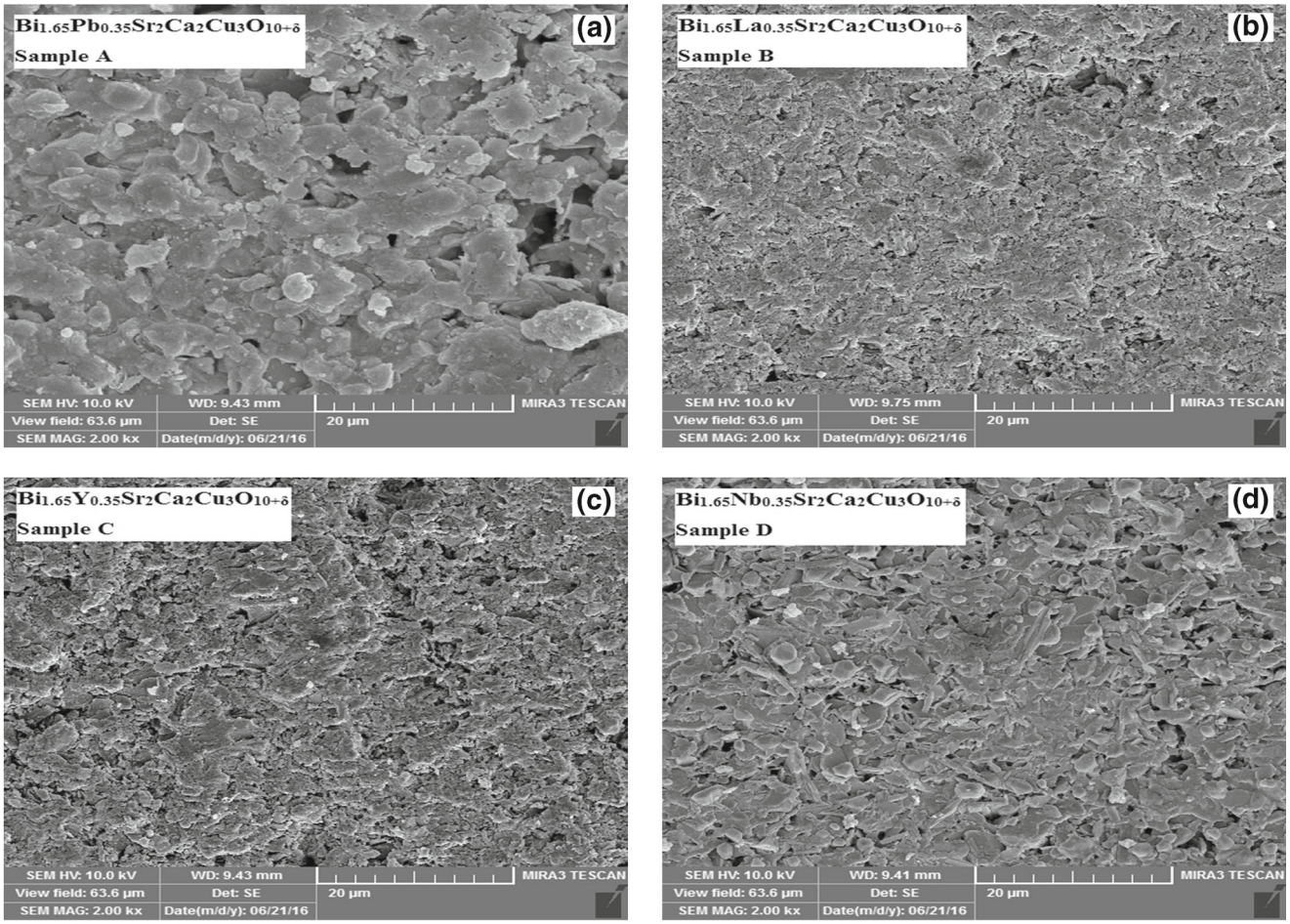

Fig. 10 SEM micrograph for samples A to D

4 Conclusion

From the results, it is revealed that the replacement of Bi^{+3} by Pb^{+2}, Nb^{+5}, Y^{+5}, and La^{+3} affected the appearance of the Bi-2223 phase and other superconducting characteristics of the samples. Among them, the sample containing Pb with the melting point of 888 °C improved the superconducting properties of the sample. Replacing Bi^{+3} by Nb^{+5}, Y^{+5}, and La^{+3} with a melting point of 1512, 2425, and 2315 °C, respectively, adversely affected the electrical and magnetic properties of BSCCO system. This negative effect grows with increasing the melting point of the replaced element The samples were sintered at the temperature of 845 °C. The substituted elements with a melting point higher than the sintering temperature not only dissolved within the main matrix to form the low-T_c (Bi-2212) phase during the sintering process but also participated in the formation of the different non-superconducting impurity phases. These results were confirmed by many kinds of experiments such as XRD, DC resistivity, and magnetic measurements. It can be concluded that in BSCCO system, to achieve a higher amount of the Bi-2223 phase, the melting point of the comprising elements must be chosen close to the sintering temperature of the samples.

Acknowledgments The authors would like to express their appreciation to Professor Ali Gencer, Center of Excellence for Superconductivity Research, Ankara University Turkey and Dr. Ramin Shiri, Iran Atomic Energy Organization, for their helpful guidance.

References

1. Maeda, H., Tanaka, Y., Fukutomi, M., Asano, T.: Jpn. J. Appl. Phys. **27**, L209 (1988)
2. Abbasi, H., Taghipour, J., Sedghi, H.: J. Alloys Compd. **494**, 305–308 (2010)
3. Özçelik, B., Kaya, C., Gündoğmuş, H., Sotelo, A., Madre, M.A.: J. Low Temp. Phys. **174**, 136–147 (2014)
4. Türk, N., Gündoğmuş, H., Akyol, M., Yakıncı, Z.D., Ekicibil, A., Özçelik, B.: J. Supercond. Nov. Magn. **27**, 711–716 (2014)
5. Özaslan, A., Özçelik, B., Özkurt, B., Sotelo, A., Madre, M.A.: J. Supercond. Nov. Magn. **27**, 53–59 (2014)
6. Gündoğmuş, H., Özçelik, B., Sotelo, A., Madre, M.A.: J. Mater. Sci: Mater. Electron. **24**, 2568–2575 (2013)
7. Özçelik, B., Özkurt, B., Yakıncı, M.E., Sotelo, A., Madre, M.A.: J. Supercond. Nov. Magn. **26**, 873–878 (2013)
8. Yazıcı, D., Özçelik, B., Yakıncı, M.E.: J. Low Temp. Phys. **163**, 370–379 (2011)
9. Abou-Aly, A.I., Abdel Gawad, M.M.H., G-Eldeen, I.: J. Supercond. Nov. Magn. **24**, 2077 (2011)
10. Abbasi, H., Taghipour, J., Sedghi, H.: J. Alloys Compd. **482**, 552–555 (2009)
11. Gao, L., Huang, J.C., Meng, L.R., Hor, H.P., Bechtold, J., Sun, Y.Y., Chu, W.C., Sheng, Z.Z., Herman, M.A.: Nature **332**, 623 (1988)
12. Chu, W.C., Bechtold, J., Gao, L., Hor, H.P., Huang, J.C., Meng, L.R., Sun, Y.Y., Wang, Y.Q., Zue, Y.Y.: Phys. Rev. Lett. **60**, 941 (1988)
13. Tallon, L.J., Buckley, G.R., Gilbert, W.P., Presland, R.M., Brown, M.W.I., Bowder, E.M., Christian, A.L., Gafull, R.: Nature **333**, 153–156 (1988)
14. Smrčková, O., Sýkorová, D., Vašek, P.: J. Superconduct.: Incorporating Novel Magnetism **13**(4), 899–901 (2000)
15. Zhigadlo, N.D., Petrashko, V.V., Saemenenko, Yu. A.., Panagopoulus, C., Cooper, J.R., Salje, E.K.H.: Phys. C Supercond. **299**(3–4), 327–337 (1998)
16. Gul, I.H., Anis-ur-Rehman, M., Magsood, A.: Phys. C Supercond. **450**(1–2), 83–87 (2006)
17. Hudakova, N., Plechacek, V., Dordor, P., Flachbart, K., Knizek, K., Kovac, J., Reiffers, M.: Supercond. Sci. Technol. **8**, 324–328 (1995)
18. Li, Y., Yang, B.: J. Mater. Sci. Lett. **13**(8), 594–596 (1994)
19. Ghazanfari, N., Kiliç, A., Gencer, A., Özkan, H.: Solid State Commun. **144**(5–6), 210–214 (2007)
20. Ekicibil, A., Coşkun, A., Özçelik, B., Kiymac, K.: J. Low Temp. Phys. **140**(1–2), 105–117 (2005)
21. Asghari, R., Arsalan, L.Ç., Sedghi, H., Naghshara, H.: Synthesis and characterization of Nb substitution on (Bi-Pb)-2223 superconductors. J. Low Temp. Phys. **189**(1–2), 15–26 (2017)
22. Asghari, R., Sedghi, H., Arsalan, L.Ç., Naghshara H: Investigation of niobium (Nb) substitution on structural and superconducting properties of (Bi, Pb)-based superconductors. Adv. Mater. Phys. Chem. **7**(7), 277–293 (2017)
23. Ismail, M., Abd-Shukor, R., Hamadneh, I., Halim, S.A.: J. Mater. Sci. **39**(10), 3517 (2004)
24. Özçelik, B., Gündoğmuş, H., Yazıcı, D.: J. Mater. Sci.: Mater. Electron. **25**, 2456–2462 (2014)
25. Türk, N., Gündoğmuş, H., Akyol, M., Yakıncı, Z.D., Ekicibil, A., Özçelik, B.: J. Supercond. Nov. Magn. **27**, 711–716 (2014)
26. Chiu, C.W., Meng, R.L., Gao, L., Huang, Z.J., Chen, F., Xue, Y.Y.: Nature **365**, 323–325 (1993)
27. Driessche, I.V., Buekenhoudt, A., Konstantinov, K., Brueneel, E., Hoste, S.: Appl. Supercond. **4**, 185–190 (1996)
28. Bean, C.P.: Rev. Mod. Phys. **36**, 31 (1964)
29. Ibrahim, M.M., Khalil, S.M., Ahmed, A.M.: J. Phys. Chem. Sol. **61**(10), 1553–1560 (2000)
30. Bahadur, D., Banerjee, A., Das, A., Gupta, K.P., Mitra, A., Tewari, M., Majumdar, A.K.: J. Mater. Sci. **25**(11), 4852–485D (1991)
31. Tampieri, A., Celotti, G., Guicciardi, S., Melandri, C.: Mater. Chem. Phys. **42**(3), 188–194 (1995)
32. Presland, M.R., Tallon, J.L., Buckley, R.G., Liu, R.S., Floer, N.E.: Physica C **176**(1–3), 95–105 (1991)
33. Obertelli, S.D., Cooper, J.R., Tallon, J.L.: Phys. Rev. B **46**, 14928–14931 (1992)
34. Sita, D.R., Singh, R.: Physica C **296**(1–2), 21–28 (1998)
35. Zhao, Z.W., Li, S.L., Won, H.H., Li, X.G.: Physica C **391**(2), 169–177 (2003)